DOI: 10.1002/ejic.200700792

(Pentamethylcyclopentadienyl)iridium-PTA (PTA = 1,3,5-Triaza-7-phosphaadamantane) Complexes and Their Application in Catalytic Water Phase Carbon Dioxide Hydrogenation

Mikael Erlandsson,[a,b] Vanessa R. Landaeta,[a][‡] Luca Gonsalvi,*[a] Maurizio Peruzzini,[a] Andrew D. Phillips,[a,b] Paul J. Dyson,[b] and Gábor Laurenczy*[b]

Keywords: Reduction / Iridium(III) complexes / Water-soluble ligands / Hydrogenation / Catalysis

The water-soluble iridium(III) complexes [Cp*Ir(PTA)Cl_2] (**1**) and [Cp*Ir(PTA)$_2$Cl]Cl (**2**) (PTA = 1,3,5-triaza-7-phosphaadamantane) have been synthesised and characterised by spectroscopy and X-ray crystallography. The complexes were evaluated as catalyst precursors for the hydrogenation of CO_2 and hydrogen carbonate in aqueous solutions, in the absence of amines or other additives, under relatively mild conditions. Complex **1** performed poorly while **2** catalyses the hydrogenation with moderate activity. The catalytically active monohydride [Cp*Ir(PTA)$_2$H]$^+$ was identified by multinuclear NMR spectroscopy and its nature confirmed by independent synthesis.

Introduction

In recent years, there has been increased concern over the emission of green house gases, and the possible consequences of these emissions.[1] Carbon dioxide is the major green house gas emission and is becoming increasingly abundant in the atmosphere. To solve the twin problems of depleting fossil fuel sources, and the associated climate change, the possibility of fixing CO_2 through catalytic hydrogenation, thereby transforming this feed-stock into an economical C_1 building block is being investigated.[2] The reduction of CO_2 through both homogeneous[3] and heterogeneous[4] catalysis has been investigated under different conditions,[5] and the use of enzymatic catalysis has also been reported.[6] However, there has been an increased interest in the development of CO_2 reduction in water[7] since CO_2 is highly soluble in water,[8] and importantly water is environmentally benign. Furthermore, it is relatively easy to recycle water-soluble catalysts from biphasic systems comprising water/organic solvents.[9] The possible primary products from the reduction of CO_2 in water include formic acid, formaldehyde, methanol and methane, but generally only the formation of formic acid is observed [Equation (1)].

$$CO_2 + H_2 \rightleftharpoons HCOOH \quad (1)$$

The catalytic hydrogenation of CO_2 in water solutions also has the advantage that the free energy for the reaction between completely dissolved reagents is slightly negative ($\Delta G° = -4$ kJ/mol), while the same gas-phase reaction between CO_2 and H_2, which produces liquid formic acid, has a positive difference in free energy ($\Delta G° = +33$ kJ/mol).[10] Moreover, when hydrogenation of CO_2 is performed in water, the CO_2/hydrogen carbonate/carbonate equilibrium has to be taken into consideration [Equation (2)].

$$CO_2 + H_2O \rightleftharpoons H_2CO_3 \rightleftharpoons HCO_3^- + H^+ \text{ [rlhar] } CO_3^{2-} + 2\ H^+ \quad (2)$$

Because of this equilibrium, the active species of the reaction may vary depending on pH, temperature and CO_2 pressure, and information concerning the identity of the active species may be provided by multinuclear NMR spectroscopy.[11] Extensive studies have been performed on the hydrogenation of CO_2 which show that the reduction is very slow at low pH, with high rates achieved around pH 8, suggesting that the actual substrate is hydrogen carbonate.[11,12] For the catalytic hydrogenation of CO_2 in aqueous solutions, complexes based on the transition metals Rh and Ru dominate, both under conventional and supercritical conditions,[13] and only a few reports have been published on the use of cyclopentadienyl iridium catalysts.[14] Recently, several papers have described water-soluble Ir and Rh cyclopentadienyl complexes and Ru arene complexes that catalyse the reduction of CO_2 and hydrogen carbonate in aque-

[a] Istituto di Chimica del Composti Organometallici, Consiglio Nazionale delle Ricerche (ICCOM-CNR),
Via Madonna del Piano 10, 50019 Sesto Fiorentino, Firenze, Italy
E-mail: l.gonsalvi@iccom.cnr.it
[b] Institut des Sciences et Ingénierie Chimiques, Ecole Polytechnique Fédérale de Lausanne (EPFL),
1015 Lausanne, Switzerland
E-mail: gabor.laurenczy@epfl.ch
[‡] Current address: Departamento de Química, Universidad Simón Bolívar,
Apartado 89000, Caracas 1080A, Venezuela
Supporting information for this article is available on the WWW under http://www.eurjic.org or from the author.

ous solution.[15] It is interesting to note that in all cases the iridium complexes perform better than the corresponding Ru and Rh complexes, indicating that studying the overlooked area of iridium-based catalysts for the reduction of bicarbonates may very well lead to the discovery of efficient catalysts for the reduction of CO_2 and hydrogen carbonate in aqueous solutions.

Herein we report the synthesis and characterisation of two novel water-soluble pentamethylcyclopentadienyl iridium complexes, bearing the water-soluble ligand PTA (PTA = 1,3,5-triaza-7-phosphaadamantane), and the results obtained using these precatalysts in the reduction of carbon dioxide and hydrogen carbonate in water.

Results and Discussion

Synthesis and Spectroscopic Characterisation

The iridium complexes used in this study were prepared from the dimer $[Cp^*IrCl(\mu\text{-}Cl)]_2$ according to the route shown in Scheme 1.

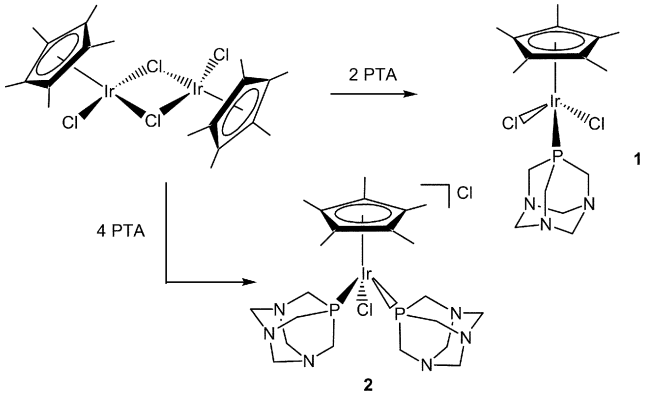

Scheme 1. Synthesis of **1** and **2**.

Direct reactions of the iridium dimer with 2 equiv. of PTA in dichloromethane (DCM) at room temperature or 4 equiv. under reflux in 2-methoxyethanol afford the water-soluble species $[Cp^*Ir(PTA)Cl_2]$ (**1**) ($S_{25\,°C}$ = 2.2 mg cm^{-3}) and $[Cp^*Ir(PTA)_2Cl]Cl$ (**2**) ($S_{25\,°C}$ = 27.5 mg of cm^{-3}), respectively. The electrospray ionisation mass spectrum (ESI-MS) of **1** in MeOH indicates the presence of the cationic species $[Cp^*Ir(PTA)Cl]^+$ (*m*/*z* = 522) with a relative intensity of 14%−the corresponding sodium adduct at *m*/*z* 544 dominates the spectrum. Compound **2** is naturally charged and in water two peaks are observed in the ESI-MS: *m*/*z* 677 (100%), corresponding to the parent cation; and *m*/*z* 659 (30%) consistent with the formation of a hydrolysis product $[Cp^*Ir(PTA)_2(OH)]^+$. The ^1H and $^{31}P\{^1H\}$ NMR spectra of **1** and **2** in CD_2Cl_2 and D_2O, respectively, agree with the proposed formulas. The methyl protons of the Cp* ring are observed at δ = 1.79 ppm as a doublet (J_{HP} = 2 Hz) for **1** and at δ = 1.84 ppm as a triplet with the same coupling constant as for **2**. Singlet resonances between 4.2 and 4.7 ppm correspond to the methylene protons within the PTA ligand, and the simple chemical shift pattern indicates a highly symmetrical conformation, suggesting that the ligand is unprotonated under these conditions.[16] The solution $^{31}P\{^1H\}$ NMR spectra of **1** and **2** exhibit singlets at –67.14 and –74.22 ppm, respectively.

Molecular Structure Determinations

Crystals of **1** and **2**, suitable for X-ray diffraction analysis, were obtained by slow evaporation from a dichloromethane/ethanol solution of **1** (Figure 1) and methanol for **2** (Figure 2). For **1**, crystallisation is accompanied by two water solvates, and for the salt **2**, the chloride anion is separated from the cation and surrounded by three methanol solvates. In compound **1**, the shortest solvate complex contact [2.00(1) Å] is between the H18B atom of water and N1 of PTA. Three cation–chloride interactions (2.704, 2.800, 2.861 Å) are observed between the methylene hydrogen atoms of the PTA ligand. The coordination sphere of the chloride anion is completed through interactions with hydroxy groups of the solvates. A strong hydrogen-bonding interaction [1.93(6) Å] between neighbouring hydroxy groups of the methanol solvates is present.

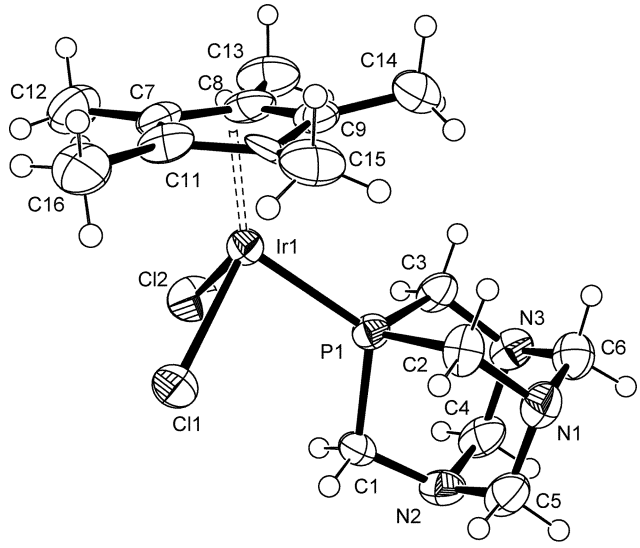

Figure 1. ORTEP diagram of **1** with solvates omitted for clarity, drawn with 50% probability ellipsoids. Selected bond lengths [Å] and angles [°]: Ir–Cp* (centroid) 1.812(5), Ir–Cl 2.418(3), Ir–P 2.274(3), P–C 1.831(11), 1.834(11), 1.848(11), (Cp*-centroid)–Ir–Cl 123.65(17), 126.83(17), Cl–Ir–Cl 87.49(11), (Cp*-centroid)–Ir–P 130.90(17), Ir–P–C 116.7(3), 119.5(3), 119.7(3), (Cp*-centroid)–Ir–P–C1: 176.7(4).

Complexes **1** and **2** have a typical piano-stool structure which is iso-structural to the recently reported rhodium analogues and forms part of an increasing family of piano-stool systems incorporating the PTA ligand.[17] Complex **2** features a longer metal–Cp* (centroid) distance [1.884(2) Å] than in **1** [1.812(5) Å]. This can be partially attributed to the greater steric influence of the second PTA group in **2**. Furthermore, a PTA-induced steric interaction with Cp* is observed with an eclipsing methyl group causing a greater bend in the C_{Me}–C_{ring}–Ir angle [C14–C7–Ir1: 131.3(8)° vs.

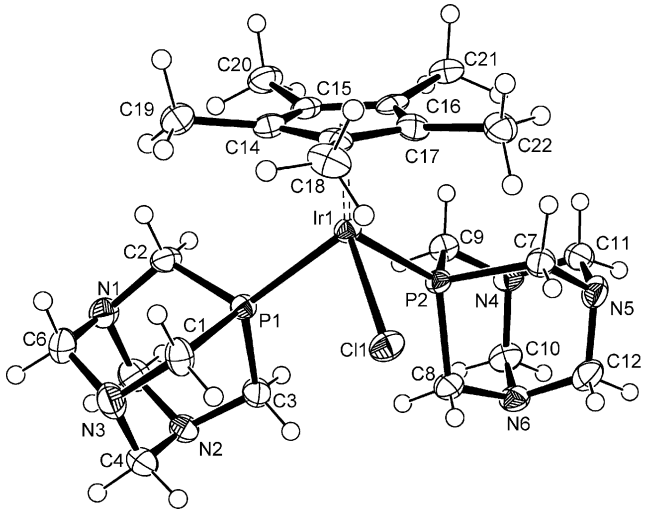

Figure 2. ORTEP diagram of **2** with solvates and anion omitted for clarity, drawn with 50% probability ellipsoids. Selected bond lengths [Å] and angles [°]: Ir–(Cp*-centroid) 1.884(2), Ir–Cl 2.429(1), Ir–P 2.308(1), 2.298(1), P–C 1.851(4), 1.839(4), 1.855(4), 1.844(4), 1.849(4), 1.869(4), Cl–Ir–(Cp*-centroid) 121.86(6), P–Ir–(Cp*-centroid) 127.12(6), 126.22(6), Cl–Ir–P 87.59(4), 84.73(4), P–Ir–P 96.62(4), Ir–P–C 119.53(13), 114.07(14), 124.27(15), 111.07(13), 122.56(14), 123.31(13), C(3,8)–P(1,2)–Ir–(Cp*-centroid) 161.3(2), 167.7(2).

C12–C7–Ir1: 125.4(8)°]. In **2**, all methyl groups are bent out of the plane, indicating increased steric strain about the metal centre. The Ir–P bond length in **1** [2.274(3) Å] is equivalent to that in $[Cp^*Ir(PMe_3)Cl_2]$ [2.281(7) Å][18] and, in general, shorter than the median value of 2.29 Å for the class of $[Cp^*Ir(PR_3)Cl_2]$ complexes which at present includes 22 examples reported in the CSD.[19] The Ir–Cl distances [both 2.418(3) Å] are also comparable to median values (2.405 Å), significantly larger than in $[Cp^*Ir(PMe_3)Cl_2]$ [2.383(7) Å, 2.388(7) Å] and more comparable to those found in $[Cp^*Ir(PPh_3)Cl_2]$ [2.406(3), 2.408(3) Å].[20] Furthermore, in comparison to $[Cp^*Ir(PMe_3)Cl_2]$ the Cl–Ir–Cl angle in **1** is smaller [87.50(9)° vs. 93.0(3)° and 90.6(1)°], but the two Cl–Ir–P bond angles are equivalent within error to those of the PMe_3-substituted complex. These data suggest that the variations in geometries are more influenced by differences in electronics between PTA and PMe_3 rather than sterics. For **2**, the Ir–Cl distance [2.429(1) Å] is only slightly longer than that in **1**. However, the Ir–P bond lengths [2.308(1) Å and 2.298(1) Å] are longer than those in **2**. A search of the CSD shows only four characterised structures where the phosphane is non-chelating.[19] A comparison of the structure $[Cp^*Ir(PMe_3)_2Cl](PF_6)$ and **2** shows comparable Ir–P bond lengths [2.290(1) Å and 2.300(1) Å],[21] but a slightly longer Ir–Cl distance [2.410(2) Å] and Ir–Cp* (centroid) [1.875(2) Å] which is probably the result of the greater donor capabilities of PMe_3 vs. PTA. Both the P–Ir–Cl [PTA: 87.59(4)°, 84.73(4)°; PMe_3: 85.81(5)°, 86.69(6)°] and P–Ir–P [PTA: 96.62(4)°; PMe_3: 96.40(5)°] bond angle are approximately equal suggesting that even though the cone angle of PTA (103°) is significantly less than that of PMe_3 (134°),[16a] steric differences between PMe_3 and PTA are less important in the bis-substituted complexes. In general, the Ir–P distances in complex **1** and **2** are shorter than those of comparable Ir species in the +1 oxidation state, reflecting the attachment of electronegative halogens and the higher oxidation state at the Ir^{III} centre.[22] In **1**, a hydrogen-bonding network is formed where the hydrogen atoms of the water solvate bridge both a chlorine [2.00(1) Å] and a nitrogen centre [2.22(1) Å], and thus a weakly bound dimeric structure is observed in the solid state (Figure 3).

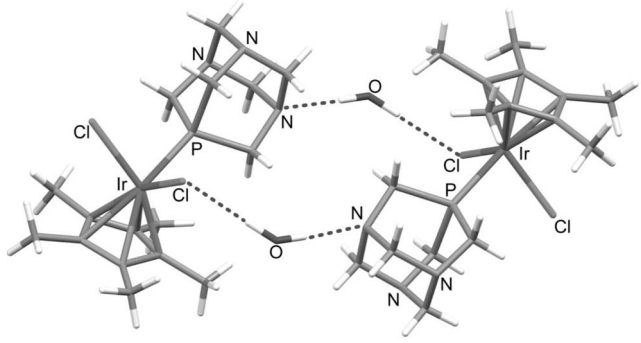

Figure 3. Ball-and-stick diagram of **1** showing the H-bonded dimer involving bridging water solvates.

Catalytic Studies

Complexes **1** and **2** were tested as catalyst precursors for the reduction of hydrogen carbonate in the pH range from 5.9 to 10.3 and in the temperature range from 70 to 100 °C under 100 bar H_2. Complex **1** proved, under the given reaction conditions, to be a poor catalyst for the hydrogenation of hydrogen carbonate, with a TOF value $<1\ h^{-1}$ at 100 °C. However, a hydride derivative of **1**, the dihydride $[Cp^*Ir(PTA)(H)_2]$ (**3**), forms quantitatively as shown by multinuclear NMR spectroscopy under the hydrogenation catalytic conditions. ^1H and ^{31}P NMR analysis of an aqueous (D_2O/H_2O, 1:4) solution of $NaH^{13}CO_3$ (0.2 M) and **1** (0.02 M), pressurised with 100 bar H_2, shows the formation of a doublet in the hydride region at $\delta = -18.4$ ppm ($^1J_{PH} = 30$ Hz) in ^1H NMR, which is simplified into a singlet in the $^1H\{^{31}P\}$ NMR spectrum (Figure 4). Accordingly, the ^{31}P NMR spectrum displays a triplet at –68.5 ppm with a $^2J_{PH} = 30$ Hz (Figure 4), which indicates, that two hydride ligands are present.

Complex **2**, on the other hand, was active and was therefore screened at different values of pH and temperature (Table 1). It was shown that **2** requires temperatures above 70 °C in order to obtain significant TOFs, and that at 80 °C the catalyst is most active in slightly basic solutions (pH 8.4–9.0).

The hydrogenation of hydrogen carbonate was followed by ^{13}C and ^1H NMR spectroscopy. A typical concentration/time profile for the formation of $HCOO^-$, monitored by ^{13}C NMR spectroscopy is shown in Figure 5.

Activation parameters for **2** were obtained by an Eyring plot of $\ln(k_{obs}/T)$ against $1/T$ (Figure 6) and the apparent

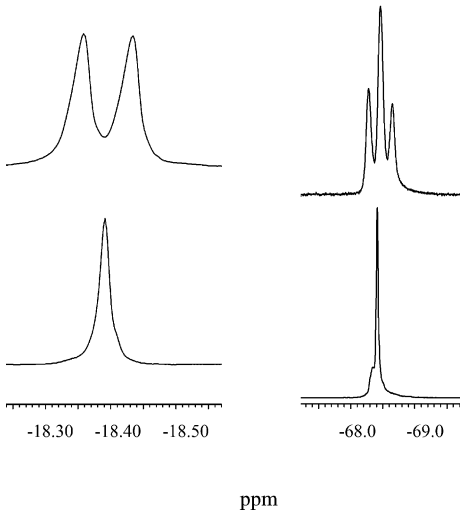

Figure 4. ^{1}H NMR (400 MHz, left) and ^{31}P NMR (162 MHz, right) spectra of the hydride region of **3**, (top left) ^{1}H, (bottom left) $^{1}H\{^{31}P\}$, δ = –18.4 ppm, $^{2}J_{HP}$ = 30 Hz; (top right) ^{31}P, (bottom right) $^{31}P\{^{1}H\}$, δ = –68.5 ppm, ($^{2}J_{HP}$ = 30 Hz). [$NaH^{13}CO_3$] = 0.24 M, pH = 8.4, $p(H_2)$ = 100 bar, [**1**] = 0.022 M, T = 20 °C.

Table 1. Catalyst screening for aqueous hydrogenation of hydrogen carbonate catalysed by **2**.[a]

T [°C]	pH	Initial TOF [h^{-1}]
70	8.4	4.0
80	8.4	10.7
90	8.4	16.5
100	8.4	22.6
80	5.9	6.5
80	9.0	12.7
80	9.2	9.1
80	9.5	6.5
80	9.8	5.4
80	10.3	2.3

[a] Conditions are provided in the Exp. Sect. Turnover frequency (TOF = mol formate/mol catalyst/h^{-1}) were calculated by non-linear least-square fits of the experimental data from the initial part of the reactions.

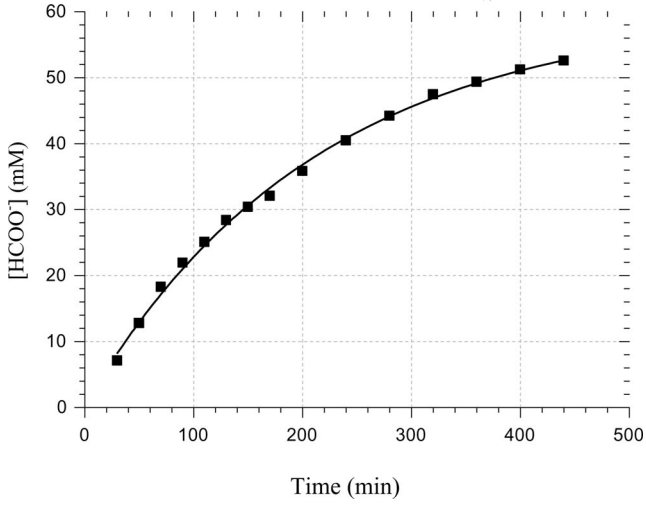

Figure 5. The initial part of the concentration/time profile for the formation of $HCOO^-$ at 70 °C, monitored in situ by ^{13}C NMR spectroscopy. Initial concentrations: [$NaH^{13}CO_3$] = 0.18 M, pH = 8.4, $p(H_2)$ = 100 bar, [**2**] = 0.0035 M.

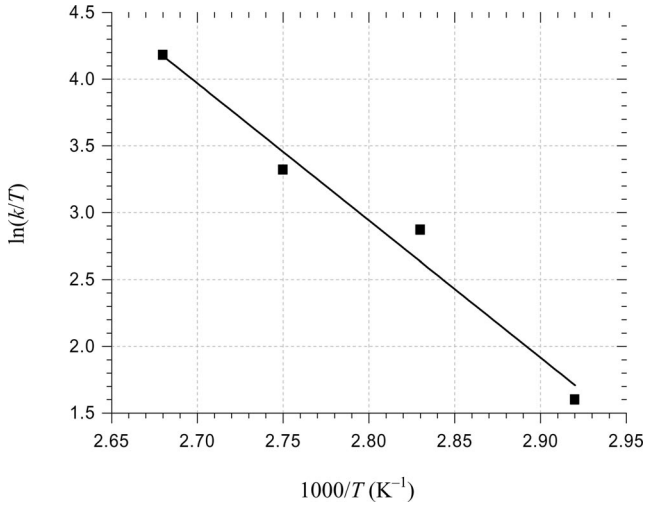

Figure 6. Eyring plot for HCO_3^- reduction catalysed by **2**.

activation enthalpy was found to be $\Delta H^{\neq}$ = +85.3 kJ mol^{-1} (the determined k_{obs} values are given in the electronic supporting information, Table S1). Although no other Ir systems bearing PTA as the ancillary ligand were reported in the literature for the reduction of carbonates, it is interesting to note that the apparent activation enthalpy obtained is very similar to that of [$RuCl_2(PTA)_4$] at + 86 kJ mol^{-1}.[11]

Tentative mechanistic information about the active catalytic species was obtained from ^{1}H NMR spectra of an aqueous (D_2O/H_2O, 1:4) solution of **2** pressurised with 100 bar H_2. The formation of the cationic monohydride [Cp*Ir$(PTA)_2H]^+$ (**4**) was evidenced by the presence of a triplet at –17.9 ppm ($^{2}J_{PH}$ = 30 Hz) simplified into a singlet by ^{31}P decoupling. The ^{31}P NMR spectrum, accordingly, shows a doublet centred at δ = –76.3 ppm with $^{2}J_{PH}$ = 30 Hz, which was again reduced to a singlet by ^{1}H decoupling. An ESI-MS of **4** in water contained the expected parent peak at m/z = 643 corresponding to 10% relative intensity, the other species present were [Cp*Ir$(PTA)_2(OH)]^+$ and [Cp*Ir$(PTA)_2Cl]^+$.

Whereas the conversion of **2** into **4** reached a maximum of ca. 15% under the conditions described, the addition of hydrogen carbonate substrate drove the reaction further and only the signal corresponding to **4** could be observed by both ^{1}H and ^{31}P NMR spectroscopy (Figure 7). In the ^{1}H spectrum, the evolution of a doublet at 9.1 ppm was also observed due to the conversion of hydrogen carbonate into formate ($^{1}J_{CH}$ = 195 Hz).

These NMR assignments were confirmed by the deliberate synthesis of **4** from the reaction between **2** and sodium formate in [D_6]DMSO (see supporting information, Figure S1).

In the ^{13}C NMR spectra, next to the resonance of free HCO_3^- at δ = 160 ppm, a signal corresponding to $[HCOO]^-$ appears (δ = 171 ppm, $^{1}J_{CH}$ = 195 Hz) together with the appearance of the ^{13}C triplet resonance of $[DCOO]^-$ (δ =

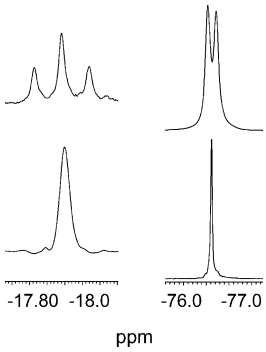

Figure 7. ^{1}H NMR (400 MHz, left) and ^{31}P NMR (162 MHz, right) spectra of the hydride region of **4**. Top left: ^{1}H; bottom left: $^{1}H\{^{31}P\}$, $\delta = -17.9$ ppm, $^{2}J_{HP} = 30$ Hz; top right: ^{31}P; bottom right: $^{31}P\{^{1}H\}$, $\delta = -79.63$ ppm, ($^{2}J_{HP} = 30$ Hz). [$NaH^{13}CO_3$] = 0.23 M, pH = 8.4, $p(H_2) = 100$ bar, **2** = 0.021 M, $T = 100$ °C.

170.8 ppm, $^{1}J_{CD} = 32$ Hz). Catalytic deuterium exchange between H_2, D_2O and formate was observed, which is not surprising as iridium phosphane complexes often catalyse H–D exchange in water.[23] Although several attempts have been made to identify the carbonate/formate intermediates by multinuclear HP NMR, none have been identified. These findings are in accordance with a recent publication where Ir-based catalysts were compared to Ru-based analogues for the reduction of CO_2 in water.[14b] The authors could identify the Ru-formate intermediate but were unable to observe the corresponding Ir-formate complex, thus concluding that the rate-determining step in the case of Ir is the reaction of the hydride complex with CO_2, whereas for the Ru catalysts it appears to be the reaction between the Ru-aqua complexes and H_2. This could also be the case in this study which would explain why only the hydride intermediate **4** could be observed. It should, however, be mentioned that both hydride and formate intermediates were unambiguously identified in a recent publication on catalytic hydrogenation of CO_2 and hydrogen carbonate in aqueous solutions using the Ru catalyst [$RuCl_2$(PTA)([9]aneS_3)], suggesting that the possibility to identify the reaction intermediates is very much dependent on the nature of the catalyst.[24]

Conclusions

Two novel pentamethylcyclopentadienyl PTA iridium complexes, i.e. [Cp*Ir(PTA)Cl_2] (**1**) and [Cp*Ir(PTA)$_2$Cl]Cl (**2**), have been synthesised in high yields and fully characterised in solution and the solid state. The two complexes were evaluated as catalysts for the hydrogenation of hydrogen carbonate in aqueous solution. While **1** proved to be essentially inactive under the reaction conditions used, the precatalyst **2** was found to be moderately active, performing best at elevated temperatures and in slightly basic aqueous solution (pH 9). Although these catalyst precursors show only moderate activity on CO_2 hydrogenation compared to similar Rh, Ru and Ir complexes,[25] they provide the possibility to analyse the reaction intermediates and mechanisms, thus contributing to further catalyst designs and reaction optimisations. It was shown by multinuclear NMR and ESI-MS, that the catalytically active species corresponds to the monohydride [Cp*Ir(PTA)$_2$H]$^+$, which was prepared and characterised independently; it appears that the η^5-C_5Me_5 ring does not dissociate from the catalyst during the reaction.

Experimental Section

General Remarks: All synthetic procedures were carried out using standard Schlenk techniques under an inert atmosphere of dry nitrogen. Solvents were distilled and degassed according to standard procedures.[26] Doubly distilled water was used throughout. Na_2CO_3 and $NaHCO_3$ (99% enriched in ^{13}C) were purchased from Cambridge Isotope Laboratories. Iridium(III) chloride, sodium 3-(trimethylsilyl)-1-propanesulfonate (TSPSA), deuterated solvents and sodium formate were bought from commercial sources and used as received. [Cp*IrCl(μ-Cl)]$_2$[27] and PTA[28] were prepared according to published procedures.

Instrumentation: ^{1}H, ^{13}C and ^{31}P NMR spectra were recorded with a Bruker DRX400 NMR spectrometer. Hydrogenation reactions were carried out in medium-pressure sapphire NMR tubes (up to 100 bar pressure) and were followed by NMR spectroscopy. TSPSA and phosphoric acid were used as references for the ^{1}H and ^{31}P NMR measurements, respectively. The spectra were fitted with WIN-NMR and NMRICMA/MALAB programs on a PC (nonlinear last squares fit to determine the spectra parameters). nESI-IT-MS analyses were performed with a Thermo Finnigan LCQ Deca XP Plus quadrupole ion-trap instrument in positive ion mode using a literature protocol.[29] The capillary temperature was set at 180 °C and the source voltage to 1.51 kV, with a mass range from 300 to 2000.

X-ray Structure Determinations: Data collection was performed with a Oxford-Diffraction XCALIBUR equipped with a Sapphire CCD area detector and graphite-monochromated Mo-K_α radiation ($\lambda = 0.71073$ Å). The crystals were kept under a 90 K gaseous flow of N_2 during the collection procedure. The unit cell and orientation matrix was determined by indexing reflections from the entire data set using CrysAlis RED.[30] All data sets are based on collecting reflections using an optimised scanning strategy utilising the programs CrysAlis CCD. After data integration with CrysAlis RED, a multi-scan absorption correction based on a semi-empirical method was applied using the MULTISCAN (part of the Platon suite) program.[31] Space group determination was performed with the XPREP program.[32] A structure solution based on the direct method algorithm was employed with SHELXS-97.[33] Afterwards, anisotropic refinement of all non-hydrogen atoms was completed based on a least-squares full-matrix method against F^2 data using SHELXL-97. Hydrogen atoms on non-solvate molecules were added through geometrically calculated positions and refined as a riding model using a scaled thermal parameter to the connecting atom. Hydrogen atoms belonging to OH groups in the solvate were located using the program Calc-OH included within the Wingx program.[34] Relevant crystallographic data for both complexes are given in Table 2 and additional specific details regarding structure refinement are available in the CIF files. Figure 1 and Figure 2) were produced with the program ORTEP-3 for Windows,[35] while for Figure 3, Mercury 1.4.2 was employed.[36]

CCDC-662262 (for **1**) and -662263 (for **2**) contain the supplementary crystallographic data for this paper. These data can be ob-

Table 2. Crystallographic data for complexes **1** and **2**.

Parameter	$[Cp^*Ir(PTA)Cl_2]\cdot 2H_2O$ = (**1**)·$2H_2O$	$[Cp^*Ir(PTA)_2Cl]Cl\cdot 2.3MeOH$ = (**2**)·2.3MeOH
Empirical formula	$C_{16}H_{31}Cl_2IrN_3O_2P$	$C_{25}H_{51}Cl_2IrN_6O_3P_2$
Formula weight	591.51	808.76
Temperature [K]	296(2)	200(2)
Crystal system	monoclinic	triclinic
Space group	$P2_1/c$	$P\bar{1}$
Crystal characteristics	orange prism	yellow prism
Crystal size [mm]	$0.80\times0.50\times0.40$	$0.50\times0.45\times0.40$
a [Å]	11.6800(10)	9.6128(5)
b [Å]	12.1934(10)	12.6200(8)
c [Å]	15.0805(13)	14.8803(8)
α [°]	90	66.771(6)
β [°]	105.955(7)	77.415(5)
γ [°]	90	76.910(5)
V [Å^3]	2065.0(3)	1598.99(16)
Z	4	2
ρ [Mg m^{-3}]	1.903	1.680
Absorption coefficient [mm^{-1}]	6.817	4.479
Collected, independent reflections	7861, 3681	14466, 5753
Collection θ range [°]	3.89–25.25	4.30–25.25
Completeness (%, θ = 25.25°)	98.3	99.5
Data	2794	5753
Restraints	12	0
Parameters	226	363
Goodness-of-fit on F^2	1.105	1.101
R_1 [$I>2\sigma(I)$], wR_2 [$I>2\sigma(I)$]	0.0508, 0.1079	0.0247, 0.0556
R_1 (all data), wR_2 (all data)	0.0761, 0.1165	0.0284, 0.0575
Max., min. residual electron density [e Å^{-3}]	2.667, –1.844	3.107, –0.838

tained free of charge from The Cambridge Crystallographic Data Centre via www.ccdc.cam.ac.uk/data_request/cif.

Catalytic Hydrogenations: In a typical reaction, $[Cp^*Ir(PTA)_2Cl]Cl$ (5.0 mg, 7×10^{-6} mol), $NaHCO_3$ (33.6 mg, 0.4×10^{-3} mol) enriched in ^{13}C, and a mixture of H_2O and D_2O (2 mL, 1:1) were introduced under a nitrogen atmosphere into a 10-mm medium-pressure sapphire NMR tube. After dissolution of all solids, the tube was pressurised with H_2 (100 bar). The tube was shaken at the desired temperature (343–373 K) using equipment built in-house. The reactions were followed in situ, the concentration of HCO_2^-, CO_3^{2-}/HCO_3^- and CO_2 were determined from the integration of the corresponding ^{13}C and ^1H NMR signals. The initial rates and turnover frequencies (TOF, given as mol formate/mol catalyst/h^{-1}) were calculated by nonlinear least-squares fit of the experimental data from the initial part of the reactions. The overall activation enthalpy was determined in the temperature range T = 343–373 K. To prepare solutions with pH < 8.3, the reaction mixture was placed in a sapphire tube and pressurised with 5 bar of CO_2. The CO_2 pressure required for obtaining a specific pH and the actual concentration of $NaHCO_3$ required to keep the total carbon concentration constant (0.2 M) were calculated using the pK values of carbonic acid, pK_1 = 6.35, pK_2 = 10.33 (at 298 K), taken from the literature.[37] In the alkaline pH-range (8.3–10.3), an appropriate mixture of Na_2CO_3 and $NaHCO_3$ was used to obtain a solution of the desired pH while keeping the total carbon concentration constant. In this pH range there is a fast exchange (on the NMR timescale) between carbonate and hydrogen carbonate, therefore an average ^{13}C NMR shift can be determined and related to the pH. ^{13}C NMR spectra were recorded before the admission of H_2, and the absolute intensity of the CO_3^{2-}/HCO_3^- signal (for pH ≥ 8.3), or the intensities of the separate HCO_3^- and CO_2 signals (slow exchange on the NMR time scale in pH <8.3 range), were used to confirm the total initial carbon concentration and to calculate the pH.[11]

Synthesis of $[Cp^*Ir(PTA)Cl_2]$ (1): To a solution of $[Cp^*IrCl(\mu\text{-}Cl)]_2$ (0.25 g, 0.31 mmol) in DCM (5 mL), solid PTA (0.1 g, 0.64 mmol) was added. The reaction was stirred at room temperature for 60 min. Ethanol (10 mL) was added and the reaction concentrated under nitrogen until an orange solid precipitated. The precipitate was filtered and washed with ice-cold ethanol (2×5 mL) and pentane (2×5 mL). The product was re-crystallised from hot ethanol. Crystals suitable of X-ray structure determination were obtained by slow evaporation from of a DCM/methanol solution of **1**. Yield: 0.32 g (92%). $C_{16}H_{27}Cl_2IrN_3P$ (555.50): calcd. C 34.52, H 4.76, N 7.36; found C 34.59, H 4.90, N 7.56. ^1H NMR (400.13 MHz, 25 °C, $CDCl_3$): δ = 1.79 (d, $^1J_{HP}$ = 2 Hz, 15 H, CH_3 Cp*), 4.31 (s, 6 H, CH_2N), 4.56 (dd, $^1J_{HP}$ = 26, $^2J_{HP}$ = 13.5 Hz, 6 H, CH_2P) ppm. $^{13}C\{^1H\}$ NMR (100.03 MHz, 25 °C, $CDCl_3$): δ = 9.33 (s, CH_3, Cp*), 49.28 (d, $^1J_{CP}$ = 22.5 Hz, CH_2P), 73.48 (d, $^2J_{CP}$ = 7 Hz, CH_2N), 92.24 (s, C_{ipso} Cp*) ppm. $^{31}P\{^1H\}$ NMR (161.98 MHz, 25 °C, $CDCl_3$): δ = –67.14 (s, 1 P) ppm. MS (nESI$^+$): m/z (%) = 521.8 $[Cp^*Ir(PTA)Cl]^+$.

Synthesis of $[Cp^*Ir(PTA)_2Cl]Cl$ (2): To a solution of $[Cp^*IrCl(\mu\text{-}Cl)]_2$ (0.25 g, 0.31 mmol) in 2-methoxyethanol (5 mL) solid PTA (0.2 g, 1.28 mmol) was added. The reaction was refluxed for 8 h. The solution was then concentrated to half of its volume, and a yellow solid precipitated. The precipitate was filtered and washed with diethyl ether (2×5 mL) and then dried under vacuum. Crystals suitable for X-ray structure determination were obtained by slow evaporation from a methanol solution of **2**. Yield: 0.40 mg (90%). $C_{22}H_{39}Cl_2IrN_6P_2$ (712.66) × $2H_2O$: calcd. C 35.42, H 5.44, N 10.87; found C 35.29, H 5.79, N 11.23. ^1H NMR (400.13 MHz, 25 °C, D_2O): δ = 1.84 (t, J_{HP} = 2 Hz, 15 H, CH_3 Cp*), 4.2–4.7 (CH_2P, CH_2N, 6 peaks, 24 H) ppm. $^{13}C\{^1H\}$ NMR (100.03 MHz, 25 °C, D_2O): δ = 9.19 (s, CH_3, Cp*), 49.53 (quint, $^1J_{CP}$ = 14, $^2J_{CP}$ = 12 Hz, CH_2P), 70.66 (t, J_{CP} = 4 Hz, CH_2N), 100.87 (t, J_{CP} = 2 Hz, C_{ipso} Cp*) ppm. $^{31}P\{^1H\}$ NMR (161.98 MHz, 25 °C, D_2O):

δ = –74.22 (s, 1 P) ppm. MS (nESI$^+$): *m/z* (%) = 677.1 [Cp*Ir(PTA)$_2$Cl]$^+$ (100%), 659.2 [Cp*Ir(PTA)$_2$(OH)]$^+$ (30%).

Synthesis of [Ir(Cp*)(PTA)$_2$H](HCO$_2$) (4): This procedure was performed in a glove box. In a 5 mL vial [Cp*Ir(PTA)$_2$Cl]Cl (25 mg, 0.035 mmol) and [D$_6$]DMSO (1 mL) were introduced. An excess of sodium formate (25 mg, 36.8 mmol), dried at 200 °C for 24 h, was added and the reaction gently heated to 100 °C whilst stirring until the yellow solution became colourless. The reaction was cooled to ambient temperature and the excess sodium formate was removed by filtration. The clear, colourless solution was transferred to an NMR tube and sealed under N_2. ^{1}H NMR (400.13 MHz, 25 °C, [D$_6$]DMSO): δ = –18.29 (t, $^2J_{HP}$ = 30 Hz, Ir-H), 2.14 (s, 15 H, CH_3, Cp*), 4.02 (s, 12 H, CH_2N), 4.50 (dd, $^1J_{HP}$ = 17, $^2J_{HP}$ = 13 Hz, 12 H, CH_2P), 8.50 (s, 1 H, $HCOO^-$) ppm. ^{13}C{^{1}H} NMR (100.03 MHz, 25 °C, [D$_6$]DMSO): δ = 11.19 (s, CH_3 Cp*), 54.67 (t, J_{CP} = 12 Hz, CH_2P), 71.95 (s, CH_2N), 98.46 (s, C_{ispo} Cp*), 166.98 (s, HCOO) ppm. ^{31}P{^{1}H} NMR (161.98 MHz, 25 °C, [D$_6$]-DMSO): δ = –77.28 (d, $^2J_{PH}$ = 30 Hz) ppm. MS (nESI$^+$) for $C_{23}H_{41}IrN_6O_2P_2$ (687.78): *m/z* (%) = 643.3 [Cp*Ir(PTA)$_2$H]$^+$ (10%), 659.2 [Cp*Ir(PTA)$_2$(OH)]$^+$ (30%), 677.1 [Cp*Ir(PTA)$_2$Cl]$^+$, 100%.

Supporting Information (see also the footnote on the first page of this article): Rate constants for the hydrogenation of hydrocarbonate under aqueous conditions catalyzed by **2**. ^{1}H- and ^{31}P-NMR spectra of **4**.

Acknowledgments

The EPFL, the Swiss State Secretariat for Education and Research (Grant SER C03.0056), COST-ESF (Action D29), and EC through projects HPRN-CT-2002-00176 (HYDROCHEM) and MRTN-CT-2003-503864 (AQUACHEM) are thanked for financial support. A. D. P. thanks the EC for a Marie Curie Intra-European Fellowship (MEIF-CT-2005-025287). M. E. thanks the foundation Bengt Lundqvist minne (Sweden) for a postdoctoral grant. Thanks are also expressed to the project Firenze Hydrolab for financial support.

[1] a) Intergovernmental Panel on Climate Change (IPCC), *Climate Change 2001: The Scientific Basis*, Cambridge University Press, Cambridge, **2001**; b) The IPCC is currently finalising its Fourth Assessment Report "Climate Change **2007**".
[2] a) A. Behr in *Carbon Dioxide Activation by Metal Complexes*, Wiley-VCH, Weinheim, **1998**; b) M. M. Halmann, M. Steinberg, *Greenhouse Gas Carbon Dioxide Mitigation: Science and Technology*, CRC Press, London, **1998**.
[3] a) J. Elek, L. Nádasdi, G. Papp, G. Laurenczy, F. Joó, *App. Catalysis A: General* **2003**, *255*, 59–67; b) P. G. Jessop, T. Ikariya, R. Noyori, *Chem. Rev.* **1995**, *95*, 259–272.
[4] A. Baiker, *Appl. Organomet. Chem.* **2000**, *14*, 751–762.
[5] a) L. D. Field, E. T. Lawrenz, W. J. Shaw, P. Turner, *Inorg. Chem.* **2000**, *39*, 5632–5638; b) W. Leitner, *Coord. Chem. Rev.* **1996**, *153*, 257–284; c) D. S. Laitar, P. Müller, J. P. Sadighi, *J. Am. Chem. Soc.* **2005**, *127*, 17196–17197; d) I. Castro-Rodriguez, K. Meyer, *J. Am. Chem. Soc.* **2005**, *127*, 11242–11243; e) W. Grochala, *Phys. Chem. Chem. Phys.* **2006**, *8*, 1340–1345.
[6] a) S. Ochoa, S. Kaufman, *J. Biol. Chem.* **1951**, *192*, 313–314; b) S. Korkes, A. Delcampillo, S. Ochoa, *J. Biol. Chem.* **1950**, *187*, 891–905.
[7] a) H. Horváth, G. Laurenczy, A. Kathó, *J. Organomet. Chem.* **2004**, *689*, 1036–1045; b) A. Kathó, Z. Opre, G. Laurenczy, F. Joó, *J. Mol. Catal. A* **2003**, *204–205*, 143–148; c) F. Hutschka, A. Dedieu, M. Eichberger, R. Fornika, W. Leitner, *J. Am. Chem. Soc.* **1997**, *119*, 4432–4443.
[8] a) V. I. Baranenko, L. N. Falkovskii, V. S. Kirov, L. N. Kurnyk, A. N. Musienko, A. I. Piontkovskii, *At. Energy* **1990**, *68*, 291–294; b) F. Mani, M. Peruzzini, P. Stoppioni, *Green Chem.* **2006**, *8*, 995–1000.
[9] D. J. Adams, P. J. Dyson, J. T. Stewart, *Chemistry in Alternative Reaction Media*, Wiley, Chichester, **2004**.
[10] P. G. Jessop, F. Joó, C.-C. Tai, *Coord. Chem. Rev.* **2004**, *248*, 2425–2442.
[11] G. Laurenczy, F. Joó, L. Nádasdi, *Inorg. Chem.* **2000**, *39*, 5083–5088.
[12] a) F. Joó, G. Laurenczy, L. Nádasdi, J. Elek, *Chem. Commun.* **1999**, 971; b) G. Laurenczy, F. Joó, L. Nádasdi, *Adv. High Pressure Res.* **2000**, *18*, 251.
[13] a) X. Yin, J. R. Moss, *Coord. Chem. Rev.* **1999**, *181*, 27–59; b) B. Cornils, W. A. Herrmann (Eds.), *Applied Homogeneous Catalysis with Organometallic Compounds*, VCH, Weinheim, **1996**, vol. 1–2.
[14] a) Y. Himeda, N. Onozawa-Komatsuzaki, H. Sugihara, K. Kasuga, *Organometallics* **2007**, *26*, 702–712; b) S. Ogo, R. Kabe, H. Hayashi, R. Harada, S. Fukuzumi, *Dalton Trans.* **2006**, 4657–4663; c) Y. Himeda, N. Onozawa-Komatsuzaki, H. Sugihara, H. Arakawa, K. Kasuga, *Organometallics* **2004**, *23*, 1480–1483.
[15] a) T. J. Geldbach, G. Laurenczy, R. Scopelliti, P. J. Dyson, *Organometallics* **2006**, *25*, 733–742; b) M. L. Man, Z. Zhou, S. M. Ng, C. P. Lau, *Dalton Trans.* **2003**, *19*, 3727–3735; c) T. A. Hanna, A. M. Baranger, R. G. Bergman, *J. Am. Chem. Soc.* **1995**, *117*, 11363–11364; d) D. J. Darensbourg, F. Joó, M. Kannisto, Á. Kathó, J. H. Reibenspies, *Organometallics* **1992**, *11*, 1990–1993.
[16] a) A. D. Phillips, L. Gonsalvi, A. Romerosa, F. Vizza, M. Peruzzini, *Coord. Chem. Rev.* **2004**, *248*, 955–993; b) C. A. Mebi, R. P. Nair, B. J. Frost, *Organometallics* **2007**, *26*, 429–438.
[17] a) A. Dorcier, P. J. Dyson, C. Gossens, U. Rothlisberger, R. Scopelliti, I. Tavernelli, *Organometallics* **2005**, *24*, 2114; b) C. Scolaro, T. J. Geldbach, S. Rochat, A. Dorcier, C. Gossens, A. Bergamo, M. Cocchietto, I. Tavernelli, G. Sava, U. Rothlisberger, P. J. Dyson, *Organometallics* **2006**, *25*, 756; c) A. Dorcier, W. H. Ang, S. Bolaño, L. Gonsalvi, L. Juillerat-Jeannerat, G. Laurenczy, M. Peruzzini, A. D. Phillips, F. Zanobini, P. J. Dyson, *Organometallics* **2006**, *25*, 4090–4096; d) W. H. Ang, E. Daldini, C. Scolaro, R. Scopelliti, L. Juillerat-Jeannerat, P. J. Dyson, *Inorg. Chem.* **2006**, *45*, 9006.
[18] F. W. B. Einstein, X. Yan, D. Sutton, *Acta Crystallogr. Sect. C: Cryst. Struct. Commun.* **1991**, *47*, 1975.
[19] F. H. Allen, *Acta Crystallogr. Sect. B* **2002**, *58*, 380–388.
[20] J. Le Bras, H. Amouri, J. Vaissermann, *J. Organomet. Chem.* **1997**, *548*, 305.
[21] R. B. Kaner, J. Kouvetakis, S. G. Mayorga, *Acta Crystallogr. Sect. C* **1986**, *42*, 500.
[22] a) D. A. Krogstad, A. J. DeBoer, W. J. Ortmeier, J. W. Rudolf, J. A. Halfen, *Inorg. Chem. Commun.* **2005**, *8*, 1141–1144; b) D. A. Krogstad, J. A. Halfen, T. J. Terry, V. G. Young, *Inorg. Chem.* **2001**, *40*, 463–471.
[23] a) G. Kovács, L. Nádasdi, F. Joó, G. Laurenczy, *C. R. Acad. Sci., Ser. IIc: Chim.* **2000**, *3*, 601–605; b) G. Kovács, L. Nádasdi, G. Laurenczy, F. Joó, *Green Chem.* **2003**, *5*, 213–217; c) S. R. Klei, J. T. Golden, T. D. Tilley, R. G. Bergman, *J. Am. Chem. Soc.* **2002**, *124*, 2092–2093.
[24] G. Laurenczy, S. Jedner, E. Alessio, P. J. Dyson, *Inorg. Chem. Commun.* **2007**, *10*, 558–562.
[25] Y. Himeda, *Eur. J. Inorg. Chem.* **2007**, 3927–3941.
[26] D. D. Perrin, W. L. F. Armarego, *Purification of Laboratory Chemicals*, 3rd ed., Pergamon Press, Oxford, **1988**.
[27] C. White, A. Yates, P. Maitlis, *Inorg. Synth.* **1992**, *29*, 228–234.
[28] D. J. Daigle, A. B. Pepperman Jr, S. L. Vail, *J. Heterocycl. Chem.* **1974**, *11*, 407–408.
[29] P. J. Dyson, J. S. McIndoe, *Inorg. Chim. Acta* **2003**, *354*, 68–74.
[30] Oxford Diffraction, *CrysAlis CCD* and *CrysAlis RED*, version 1.71, Oxford Diffraction, Abingdon, **2006**.

[31] A. L. Spek, *PLATON*, A Multipurpose Crystallographic Tool, Utrecht University, **2005**.
[32] Bruker-Nonius, *XPREP*, Reciprocal Space Exploration, version 6.14, Bruker AXS, Madison, Wisconsin, **2003**.
[33] G. M. Sheldrick, *SHELXL-97*, A Program for the Refinement of Crystal Structures, Release 6, University of Göttingen, **2003**.
[34] M. Nardelli, *J. Appl. Crystallogr.* **1999**, *32*, 563–571.
[35] F. J. Farrugia, *J. Appl. Crystallogr.* **1997**, *30*, 565.
[36] C. F. Macrae, P. R. Edgington, P. McCabe, E. Pidcock, G. P. Shields, R. Taylor, M. Towler, J. van de Streek, *J. Appl. Crystallogr.* **2006**, *39*, 453–457.
[37] D. R. Lide (ed.), *CRC Handbook of Chemistry and Physics*, CRC Press, Boca Raton, FL, 84th ed., **2004**.

Received: July 26, 2007
Published Online: Decmeber 3, 2007

